Impact of Transmitter and Receiver Imperfections on the Performance of Coherent Optical QPSK Communication Systems

(1):C. S. Petrou, A. Vgenis, A. Kiourti, I. Roudas, (2):J. Hurley, M. Sauer, J. Downie, Y. Mauro, and S. Raghavan
(1): Electrical & Computer Engineering, University of Patras, Rio, 26500, Greece; petrou@ece.upatras.gr;
(2): Corning Inc., Corning, NY 14831, USA; raghavans@corning.com

Abstract

We investigate transmitter and receiver imperfections in coherent QPSK systems, and how their impact can be mitigated using DSP algorithms. Quadrature imbalance was found to be a particularly significant effect that will require compensation.

Introduction

Quadrature Phase Shift Keying (QPSK) has attracted considerable attention recently, partly due to its superior theoretical spectral efficiency compared to conventional binary On-Off-Keying (OOK) [1], and partly due to its increased transmission impairment tolerance. Homodyne detection of this modulation format, apart from its well-known sensitivity and selectivity, enables efficient digital signal processing (DSP), stemming from the linear nature of the receiver [2]. In this paper, we investigate the impact of transmitter and homodyne receiver imperfections on the performance of optical QPSK communication systems, performing a series of 10 GBd back-to-back experiments. Two 90° optical hybrids are used in the study. Quadrature Imbalance (QI) arising from imperfections of the 90° optical hybrid [3] is found to be a ubiquitous and significant impairment. In addition, intermediate frequency (IF) offset and modulation waveform ripple are found to be non-negligible. We propose a QI estimation and compensation algorithm and examine its performance combined with Feed Forward Frequency Estimation (FFFE) [4] and Adaptive Equalization (AE) [5].

Experimental setup

Fig. 1a shows the block diagram of the experimental setup used for the current study. Light from an external cavity laser (ECL), acting as a transmitter, is QPSK modulated using a quadrature modulator (QM), driven by two 10 Gb/s pseudo-random bit sequences (PRBS). The optical signal passes through a variable optical attenuator (VOA) to emulate fiber attenuation. The received optical signal, after passing through a Polarization Beam Splitter (PBS), is combined with the light of an ECL, acting as a local oscillator (LO), in a bulk 2×2 90° optical hybrid [6] and an integrated 2×4 90° optical hybrid [2]. At the output of the 2×2 90° optical hybrid, two, approximately matched, fast photodiodes (PD) are used. The integrated 2×4 90° optical hybrid is followed by two approximately balanced photodiodes (BPD). Finally, an 8-GHz electrical bandwidth, 40 GSa/s, real-time, sampling oscilloscope samples the photocurrents and stores the signal for off-line processing (Fig. 1b). An electrical spectrum analyzer, not shown in Fig. 1a, is used for the manual adjustment of the transmitter and LO frequencies. The duration of a single measurement is equal to 51.25 μs.

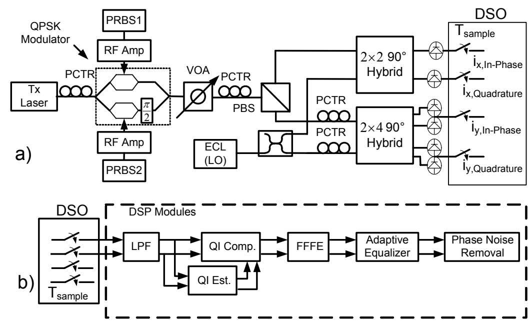

Fig. 1 a) Experimental setup (Abbreviations: Tx Laser = Transmitter Laser, PRBS = Pseudo-Random Bit Sequence, RF Amp = Radio Frequency Amplifier, PCTR = Polarization Controller, VOA = Variable Optical Attenuator, PBS = Polarization Beam Splitter, DSO = Digital Sampling Oscilloscope, LO = Local Oscillator), b) DSP modules.

System imperfections and DSP modules

The impact of each transmitter and homodyne receiver imperfection on received constellation diagrams can be visualized separately, using simulation. In Fig. 2a, the ideal constellation, when no impairments are present, is shown. PRBS voltage waveforms are found to exhibit non-negligible ringing at the upper trace. Non-ideal NRZ pulses, driving the QPSK modulator, lead to erroneous phase variations at the QM output. The received constellation is thicker in the upper right quadrant (Fig. 2b). At the receiver front-end, inaccuracies in the bias voltages of the 2×4 90° hybrid, in conjunction with non-balanced PDs, as well as non-optimal setting of the four polarization controllers within the 2×2 90° optical hybrid, cause QI (Fig. 2c). In the frequency domain, the presence of QI contaminates the single sideband IF spectrum produced by the phase-diversity receiver with an attenuated image of the unwanted sideband, which leads to a degradation of the system performance [7]. In the time domain, QI tilts and squeezes the square constellation into a diamond shape. On the other hand, phase noise dithers the constellation points and transforms them into arcs (Fig. 2d for 300 kHz total 3-dB linewidth). Furthermore, IF offset continuously rotates the constellation. In the presence of all aforementioned imperfections, the constellation becomes elliptical, and slightly thicker in one of the quadrants (Fig. 2e). Finally, Fig. 2f shows a typical experimental constellation diagram, manifesting all these effects.

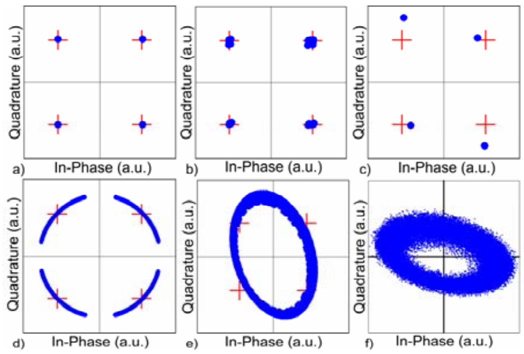

Fig. 2 a) Ideal constellation, b) Impact of PRBS ripple, c) Impact of QI, d) Impact of phase noise, e) Impact of all impairments in the presence of IF, f) Typical experimental constellation. Crosses: ideal points.

Compensation of the various transmitter and receiver imperfections is performed by a sequence of distinct DSP modules (Fig. 1b). First, electronic lowpass filtering (LPF) with a 3-dB bandwidth equal to 0.8 times the symbol rate R_S, is performed. Then, for QI estimation, a least-squares algorithm is used for fitting the constellation to an ellipse [8]. Ellipse parameters are extracted, namely its center (x_0, y_0), its maximum values in both axes (x_{max}, y_{max}) and its angle of rotation α. From these, the fractional amplitude imbalance ε and phase imbalance φ [9], are derived. Since QI imbalance is constant during a single measurement, only a small number of symbols is required for its estimation. Given ε and φ, QI compensation is performed using a linear transformation [9], which transforms the ellipse into a circle. Subsequently, the bulk of IF offset is estimated and removed using a FFFE algorithm [4]: first, the complex symbols constructed from the samples of the photocurrents are raised to the fourth power to eliminate phase modulation, and then IF offset is derived by calculating the mean phase change between neighbouring symbols. Adaptive equalization of the remaining distortions of the received signal is performed by an adaptive complex T/2 fractionally-spaced linear filter [5]. Finally, a symbol-by-symbol phase noise-removing unit is used [5], which can additionally remove any remaining IF offset. Not compensating for QI results in inferior performance or even complete failure of all subsequent modules.

Experimental results

In all experiments QI was noticeable for both optical hybrids. In Fig. 3 we present experimental data from the output of the 2×2 90° optical hybrid. Fig. 3a and 3d show constellation diagrams for a small and a large QI case, respectively. Fig. 3b and 3e correspond to the output of the AE module for the two aforementioned cases, when no prior QI compensation is performed. Large QI prevents the AE module from functioning properly. Fig. 3c and 3f correspond to the output of the AE module when QI compensation is performed. In the first case, QI compensation only slightly improves the quality of the constellation, while in the latter, its use is imperative. In both cases, an IF offset around 200 MHz was estimated and removed with the FFFE.

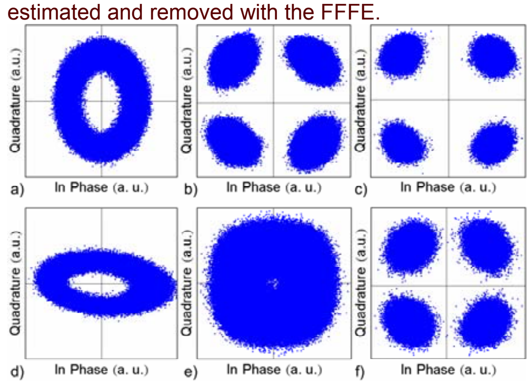

Fig. 3 Constellations at the input and output of the DSP section, with and without QI compensation, for experiments featuring non-intentional QI.

Conclusions

Performance of a fractionally-spaced AE algorithm is limited by QI, an inevitable, occasionally severe, receiver imperfection. We propose a QI compensation algorithm that eliminates this impairment.

References

1. J. M. Kahn et al., IEEE J. Sel. Topics Quantum Electron., pp. 259–272, Mar. 2004.
2. R. Noé, IEEE J. Lightw. Technol., pp. 802–808, Feb. 2005.
3. C. S. Petrou et al., CLEO'08, paper CThJJ1.
4. A. Leven et al., IEEE Photonics Technol. Lett, pp. 366–368, Mar. 2007.
5. D. Crivelli et al., GLOBECOM' 04, pp. 2545–2551.
6. L. G. Kazovsky et al., Appl. Opt., pp. 366–368, Feb. 1987.
7. M. Valkama et al., IEEE Trans. Signal Process, pp. 2335–2344, Oct. 2001.
8. R. Halíř et al., Proc. Int. Conf. in Central Europe on Computer Graphics, Visualization and Interactive Digital Media, pp. 125–132, 1998.
9. F. E. Churchill et al., IEEE Trans. Aerosp. Electron. Syst., pp. 131–136, Jan. 1981.